Advances in Concrete Construction, *Vol. 6, No. 5 (2018) 485-507*
DOI: https://doi.org/10.12989/acc.2018.6.5.485

Residual strength capacity of fire-exposed circular concrete-filled steel tube stub columns

Ihssan A. Alhatmey*, Talha Ekmekyapar and Salih K. Alrebeh

Department of Civil Engineering, University of Gaziantep, 27310 Gaziantep, Turkey

(Received July 12, 2018, Revised August 6, 2018, Accepted August 9, 2018)

Abstract. Concrete-Filled Steel Tube (CFST) columns are an increasingly popular means to support great compressive loads in buildings. The residual strength capacity of CFST stub columns may be utilized to assess the potential damage caused by fire and calculate the structural fire protection for least post-fire repair. Ten specimens under room conditions and 10 specimens under fire exposure to the Eurocode smouldering slow-growth fire were tested to examine the effects of diameter to thickness D/t ratio and reinforcing bars on residual strength capacity, ductility and stiffness of CFST stub columns. On the other hand, in sixteen among the twenty specimens, three or six reinforcing bars were welded inside the steel tube. The longitudinal strains in the steel tube and load-displacement relationships were recorded throughout the subsequent compressive tests. Corresponding values of residual strength capacity calculated using AISC 360-10 and EC4 standards are presented for comparison purposes with the experimental results of this study. The test results showed that after exposure to 750°C, the residual strength capacity increased for all specimens, while the ductility and stiffness were slightly decreased. The comparison results showed that the predicted residual strength using EC4 were close to those obtained experimentally in this research.

Keywords: circular CFST stub columns; post-fire residual strength; welded reinforcing bars; design specifications

1. Introduction

Concrete filled steel tube (CFST) stub columns integrate the appropriate characteristics of concrete and steel materials, therefore providing the advantages of high ductility, high stiffness and strength, great energy dissipation, considerable economy and high speed of construction (Tao *et al*. 2009). For this reason, CFST have been utilized widely in numerous countries in recent decades. CFST stub columns with reinforcing bars inserted and welded inside steel tubes have several benefits. The main benefit is a substantial increase in load bearing capacity of the columns due to the reinforcing bars and concrete filling. In addition, circular CFST columns that are filled with reinforced concrete enhance the structural fire resistance and provide superior load carrying capacity as compared with unfilled steel tubes. CFST also have much better endurance characteristics and advantages than conventional reinforced concrete columns during and under fire conditions as the steel tube prevents spalling of the concrete which remains protected against fire. Moreover, the

*Corresponding author, Ph.D. Student, E-mail: ia68679@mail2.gantep.edu.tr, alrekabi2017@gmail.com

http://www.techno-press.org/?journal=acc&subpage=7 ISSN: 2287-5301 (Print), 2287-531X (Online)

tube form of the steel eliminates the need for formwork. These benefits have led to the increased utilization of such columns in some of the recent high-rise buildings in China, as well as in other countries.

Previous studies, presented by (Han *et al*. 2002, Han and Huo 2003, Han *et al*. 2005) conducted analysis and tests of greater than 40 CFST columns after exposure to fire, and have also proposed complex post-fire material models for predicting CFST columns' residual capacity. Their work includes post-fire exposure residual tests on both unprotected and protected scaled CFST columns. In addition to the specimens tested without exposure to high temperature, all their rest specimens were exposed to 900℃. The tested specimens were either circular or square columns with maximum cross-sectional dimensions between 80 and 133 mm and lengths ranging between 380 and 1200 mm.

Yang *et al*. (2008) conducted a number of experimental studies on residual strength of material models and proposed predictive equations for the residual strength of both protected and unprotected (with a specified cementitious protection material) CFST columns after exposure to the fire. In the previous studies, although there are a big number of research studies on realistic performance of real fire conditions, such as (Kodur 1999, Kim *et al*. 2000, Kodur and Sultan 2000, Han 2001, Renaud *et al*. 2003, Park *et al*. 2008, Tao *et al*. 2011, Rush *et al*. 2012, Choi *et al*. 2012, Zaharia and Dubina 2014, Zhang *et al*. 2014, Shaikh and Taweel 2015, Zhang *et al*. 2016, Ada *et al*. 2018), there is little research work on behavior of post-fire of composite columns.

The residual strength capacity of CFST columns may be utilized to assess the potential damage caused by fire and calculate the structural fire protection for least post-fire repair. It can be concluded from briefly reviewed literature that none of the previous researches dealt with reinforcing bars welded to the steel tube. This paper presents tests on the post-fire residual compressive load capacity of ten CFST stub columns after exposure to the smouldering fire curve (2010) in addition to ten unheated control columns. All reinforcing bars were welded to inside perimeter of the steel tubes. The considered parameters in this study are the *D/t* ratio, the diameter of the welded reinforcing bars, and the number of these bars.

The diameter and number of welded reinforcing bars significantly improves the toughness, ductility and compression performance of the columns. Considering different (*D/t*) ratios utilized in this research, it has been shown that welded reinforcing bars can be used for thicker and thinner steel tubes which are filled with concrete. Nevertheless, further experimental studies are required considering different *D/t* ratios to assess the performance of the welded reinforcing bars performance for wider range of investigated parameters before, during and after exposure to the fire. Using vertically welded reinforcing bars in CFST stub column applications would result in cost effective and reliable designs, provided that a suitable weld plan is followed.

2. Experimental program

Twenty CFST specimens were fabricated and tested in this research. Ten specimens were tested after exposure to the fire test reaching heating temperature of 750℃, while the other test specimens were tested without exposure to high temperatures. All specimens were tested at room temperature under concentric compression until failure. The following sections detail the experimental program conducted in this study.

2.1 Column specimens

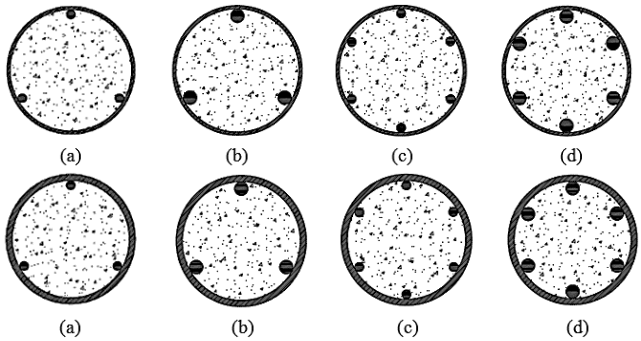

Fig. 1 Layouts of reinforcing bars with 3.15 and 5.63 mm wall thickness: (a) 3-Ø 8; (b) 3-Ø 12; (c) 6-Ø 8; and (d) 6-Ø 12

Table 1 Details of stub column specimens

Column no.	D (mm)	t (mm)	f_c (MPa)	f_y (MPa)	f_{ysr} (MPa)	N_{exp} (kN)	Reinforcing bars	t_h (min)
3-Ø 8	114.3	3.15	50.83	460	534	1170.47	3Ø 8	0
6-Ø 8	114.3	3.15	50.83	460	534	1257.89	6Ø 8	0
3-Ø 12	114.3	3.15	50.83	460	470	1230.99	3Ø 12	0
6-Ø 12	114.3	3.15	50.83	460	470	1455.33	6Ø 12	0
C	114.3	3.15	50.83	460	-	1060.59	-	0
T-3-Ø 8	114.3	5.63	49.59	410	534	1486.99	3Ø 8	0
T-6-Ø 8	114.3	5.63	49.59	410	534	1573.58	6Ø 8	0
T-3-Ø 12	114.3	5.63	49.59	410	470	1554.41	3Ø 12	0
T-6-Ø 12	114.3	5.63	49.59	410	470	1796.96	6Ø 12	0
T-C	114.3	5.63	49.59	410	-	1358.71	-	0
F-T-3-Ø 8	114.3	3.15	50.83	460	534	1243.38	3Ø 8	60
F-T-6-Ø 8	114.3	3.15	50.83	460	534	1361.01	6Ø 8	60
F-T-3-Ø 12	114.3	3.15	50.83	460	470	1357.57	3Ø 12	60
F-T-6-Ø 12	114.3	3.15	50.83	460	470	1560.59	6Ø 12	60
F-T-C	114.3	3.15	50.83	460	-	-	-	60
F-T-T-3-Ø 8	114.3	5.63	49.59	410	534	1598.73	3Ø 8	60
F-T-T-6-Ø 8	114.3	5.63	49.59	410	534	1717.23	6Ø 8	60
F-T-T-3-Ø 12	114.3	5.63	49.59	410	470	1683.01	3Ø 12	60
F-T-T-6-Ø 12	114.3	5.63	49.59	410	470	1869.41	6Ø 12	60
F-T-T-C	114.3	5.63	49.59	410	-	-	-	60

*F-T: Fire test; T: Tube thickness; 6-Ø 12: Number and diameter of welded reinforcing bars; t_h: Heating time to the maximum fire temperature.

All of the specimens were manufactured using 270 mm length steel tubes which corresponds to a stub column configuration (Ekmekyapar and ALEliwi 2017). Since the global failure mode is prevented in stub columns, mechanical properties of materials could be effectively exploited. Each circular tube of CFST column was fabricated by welding several reinforcing bars to the inside diameter of the steel tube. Sixteen specimens were fabricated with welded reinforcing bars, while the other four specimens were fabricated without reinforcing bars. Considering the diameter-to-

thickness (*D/t*) ratio as an investigated parameter, ten specimens were fabricated using steel tube thickness of 3.15 mm, while the thickness of the steel tubes of the rest ten specimens was 5.63 mm. The thickness of the fabricated specimens and the details of the welded bars are shown in Fig. 1. Table 1 lists the properties of the steel tubes and the reinforcing bars. The properties of the tube were chosen to allow various kinds of failure behaviors to occur under compression loading. Details and properties of the CFST stub columns are also presented in Table 1.

Employed column specimens naming system in Table1 includes the tube thickness (*t*), concrete strength (*fc*) and circular tube diameter (*D*), respectively. For example, the specimen F-T-T-6-Ø 12 represents CFST stub column with (F-T) referring to fire test, (T) refers to tube thickness and 6-Ø 12 refers to the number and diameter of welded reinforcing bars. A typical cross-section is shown in Fig. 2. Before casting the concrete, the upper and lower ends of the tubes were machined to assure maximum uniformity of contact with the heads of the loading of the testing machine (Ekmekyapar 2016, Ekmekyapar and Al-Eliwi 2016). Providing the flatness and uniformity of specimen ends is a crucial step in tube specimen procedure of testing to gain very reliable test results (Ziemian 2010). Fig. 3 illustrates the process of machining of tubes.

In order to provide suitable interaction and coherence between the concrete and the steel tubes, internal surfaces of the circular tubes were cleaned thoroughly from dust. Also, in order to restrict the concrete during casting, mica plates were utilized at the base ends of the steel tubes. Silicon was utilized to relate the mica plates to the base ends of tubes. There was no connect between concrete and mica plates, so that the smooth surfaces of core concrete at the base ends of the tubes were obtained facilely when removing the thick mica material. The concrete inside the steel tubes was cast in several layers. The top 10 mm of the tubes were left empty without concrete for leveling purposes of specimens prior to testing.

2.2 Material properties

Nowadays, there is a growing very interest in utilizing self-consolidating concrete (SCC) in the construction of CFST. Known as a type of high performance concrete, SCC can fill in formworks without the requirement of any external and internal vibration. The utilization of SCC in construction can reduce labor cost, shorten construction periods and improvement compaction

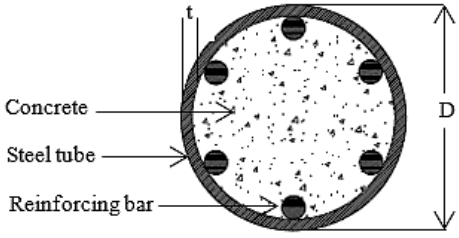

Fig. 2 Typical cross-section of columns

Fig. 3 Machining of steel tubes

Fig. 4 The utilized furnace

Fig. 5 Setup of column specimens inside the furnace before exposure to fire

quality particularly in restricted and confined areas where compaction is very difficult. Also, in this test program, a SCC mixture was used to fill the tubes. To evaluate the concrete compressive strength 100×200 mm cylinders were utilized. Considering the size of tubes, maximum diameter of coarse aggregate of 10 mm was used, while class (F) fly ash (FA) and fine aggregate (sand) were utilized in the concrete mixture. After the curing period, the concrete compressive strength was tested in accordance with ASTM C39/C39M (2014).

The measured compressive strength of all specimens was in the range of 49.59 MPa to 50.83 MPa. The yield strength values of the steel tubes and the longitudinal reinforcing bars are listed in Table 1.

2.3 Heat treatment

After being treated for about 1 month, the corresponding columns were heated using an electrical furnace for the purpose of drying at the Structural Laboratory of Gaziantep University, Turkey. Ten specimens were dried for 48 hours at 100℃ before the high temperatures are applied. It is worthy to mention here that increasing the fine particles in the mixture would reduce the link between the pores or reduce the porosity, which increases the pore water pressure growth. Therefore, the preheating to 100℃ reduces the free water in the concrete pores but not expel it all. The dimensions of the furnace were 620 ×1300 ×1360 mm and it is of 1200℃ capacity, as shown in Fig. 4. Electrical heaters are installed on five sides, except the floor of the furnace to ensure that the heat is applied homogenously on the heated columns. The temperature of the furnace is measured using type-K thermocouples. Before exposure to the fire, both ends of the columns were covered by a layer of mineral wool, as shown in Fig. 5. This procedure was applied to decrease the heat transfer from the column ends to the interface of steel-concrete. The furnace heating was controlled as closely as possible to the smouldering fire curve, as shown in Fig. 6. However, the fire duration time T was set to be 60 min, leading to a goal furnace temperature of 750℃ at the end of the fire test. At the end of the heating period, the furnace and specimens were cooled down smoothly by opening the cover of ventilation at the roof of the furnace as shown in Fig. 4. The gradual cooling stage aimed to prevent the effect of sudden difference in thermal strains due to sharp temperature drop produced from sudden cooling.

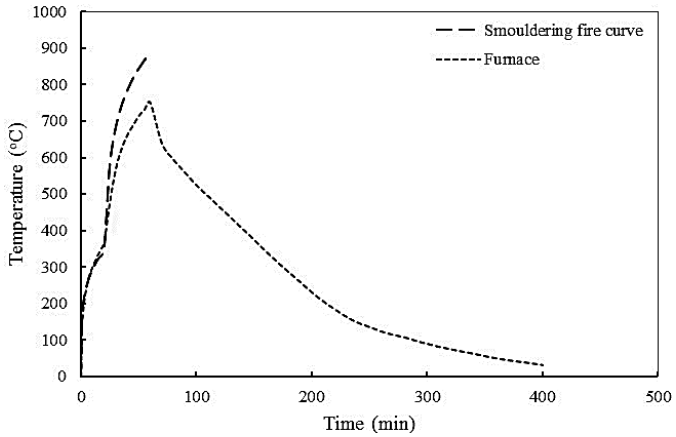

Fig. 6 Comparisons of measured furnace temperature with smouldering fire curve at 60 min

Fig. 7 Specimens ready for testing

Fig. 8 Testing of column specimens

2.4 Test setup and instrumentation

After finishing the heat treatment, the top of the steel tubes was leveled utilizing (high strength leveling) epoxy. Fig. 7 shows eighteen CFST stub columns, which are prepared and ready for testing. CFST stub columns were centered in the testing machine very carefully to eliminate the possibility of eccentric loading. A 2500 kN hydraulic compression machine was utilized to conduct the tests. The column was inserted in the compression machine in a vertical position. A steel block was placed between the top platen of the compression machine and the specimen. The steel block has a cross-section which is a little greater than that of the specimen. Fig. 8 illustrates a displacement controlled compressive loading with a rate of about 0.5 mm/min was applied to all columns up to the end of the tests. Axial strains in the tube were measured utilizing installed strain gauges on the middle of the tubes. It is possible to analyze the load transfer mechanism from the concrete to the steel tube depending on the strain readings. In addition, Fig. 8 illustrates LVDT 1 and LVDT 2 that were utilized to monitor the axial deformation of the tested steel tube.

3. Experimental results and discussions

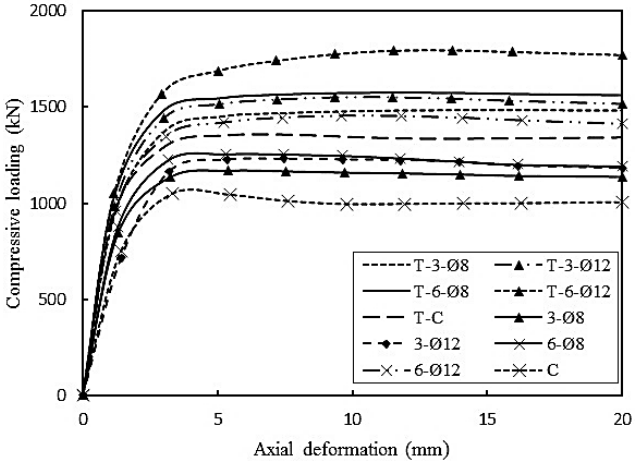

Fig. 9 Compressive loading versus axial deformation curves of columns without fire exposure

3.1 CFST stub columns without fire exposure

The compressive loadings versus axial deformation curves of CFST stub columns are presented in this section to discuss the load resistance, ductility and stiffness behaviors of the columns. The influence of each of the investigated parameters, including the properties of the reinforcing bars, steel tube and core concrete, on the behavior of the tested columns is addressed. Compression loadings versus axial deformation curves of the composite columns without fire exposure are presented in Fig. 9.

Specimen C, which composes of unreinforced thin tube, achieved a compression load capacity of 1060.6 kN with good ductility behavior. It is worth to note that all column specimens without fire exposure in this set of CFST stub columns exhibited high ductility as shown in Fig. 9. Compression capacities of the CFST specimens with 3-Ø 8 and T-6-Ø 12 were recorded to be 1170.5 and 1797 kN, respectively. Considering the capacity of the specimen C, the accumulated effect of the examined CFST stub column parameters (tube thickness, bar diameter and bar number) provided a performance increases in the range of 10.4 to 70%. These levels of performance increase are significant and show the effectiveness of CFST concept.

Examining the influence of CFST stub column parameters, it can be surely deduced that the most effective component is the welded reinforcing bars. For the same tube thickness, the increment in diameter and numbers of the reinforcing bars in CFST stub column without fire exposure led to 37.2% capacity improvement (comparison of C with 6-Ø 12), whereas this improvement was only 28.1% when the thickness of the tube was increased for specimens having no steel bars (comparison of C and T-C).

3.2 CFST stub columns after fire exposure

Figs. 10 and 11, illustrate the compression loading versus axial deformation curves of columns before and after fire exposure. The compression capacity of the specimen F-T-3-Ø 8 was 1243.4 kN. Although specimen F-T-3-Ø 8 has 6.2% greater compression capacity compared to the specimen 3-Ø 8, specimen 3-Ø 8 showed a superior ductility performance as shown in Fig. 10. The

hydraulic configuration of the testing machine does not allow the specified displacement rate to be followed after 2300 kN due to safety reasons, therefore, the tests were terminated when the ultimate load reached 2300 kN. The CFST columns F-T-6-Ø 8, F-T-3-Ø 12, F-T-6-Ø 12, F-T-T-3-Ø 8, F-T-T-6-Ø 8, F-T-T-3-Ø 12 and F-T-T-6-Ø 12 developed compression load capacities of 1361, 1357.6, 1560.6, 1598.7, 1717.2, 1683 and 1869.4 kN, respectively. Therefore, the CFST stub column after fire exposure exhibited performance increments in the range of 9.2% and 50.3% compared to performance of the specimen F-T-3-Ø 8. As expected, the compression load capacities of CFST stub columns after fire exposure were greater than the corresponding CFST stub columns before fire exposure. However, the percentage increase obtained for columns without fire exposure are greater as detailed in section 3.1. It should also be noted that the specimens before fire exposure have greater initial stiffness and ductility compared to the stiffness and ductility of the specimens after fire exposure, as shown in Figs. 10 and 11.

Comparison of the performances of CFST stub columns before fire exposure and their corresponding CFST stub columns after fire exposure reveals important understandings. The specimen F-T-3-Ø 8 has 73 kN greater load capacity compared to the capacity of the specimen 3-Ø 8 which corresponds to a 6.23% performance increment. However, the specimens F-T-6-Ø 8, F-T-3-Ø 12, F-T-6-Ø 12, F-T-T-3-Ø 8, F-T-T-6-Ø 8, F-T-T-3-Ø 12 and F-T-T-6-Ø 12 achieved 103.1, 126.6, 105.3, 111.7, 143.6, 128.6 and 72.4 kN greater compression capacities compared to the capacities of their corresponding unheated specimens. It is worth to note here, that the use of type F fly ash enhances the compressive strength of concrete after exposure to high temperatures. In this research, where the used concrete incorporates type F fly ash, it was found that the load resistances of specimens exposed to 750℃ were higher than those of corresponding unheated specimens, the reason was type F fly ash increasing compression load capacity of CFST stub columns.

Increasing of compressive strength after exposure to high temperatures agrees with findings of previous researches (Rashad and Zeedan 2011, Zhang *et al*. 2014, Ibrahim *et al*. 2012). Zhang *et al*. (2014) found that the compressive strength is lost after exposure to 500℃ for specimens with low fly ash content (0% and 20%), while specimens with higher fly ash content 50%, 75% and 100 % exhibited higher compressive strength retention. Ibrahim *et al*. (2012) also confirmed that fly ash incorporation increases the residual compressive strength after exposure to temperatures up to 700℃.

Many chemical and physical factors related to both cementitious materials (fly ash+cement) and aggregate lead to the increase of compressive strength of concrete after exposure to high temperatures. Recalling the mix design of the current study, the percentage volume of coarse aggregate is much less than of fine aggregate, which increases the surface area that absorbs the free water uniformly and effectively. Thus, produces a matrix with more homogenous particle distribution. Furthermore, increasing the graded fine particles reduces the pores and envelopes the coarse aggregate actively, which enhances the bond between the coarse aggregate and other materials. Consequently, such factors lead to better distribution of stresses and hence reduce the stress localization. In this study, this activity was more obvious after exposure to high temperatures, as shown in Figs. 10 and 11.

The existence of the welded reinforcing bars significantly improves the toughness and ductility behaviors of the columns. The characteristics of the compression loading versus axial deformation curves in Figs. 10 and 11 show the significant contribution of the welded reinforcing bars to the toughness and ductility of the tested specimens. Furthermore, the deformation responses of the CFST stub columns before and after fire exposure are different.

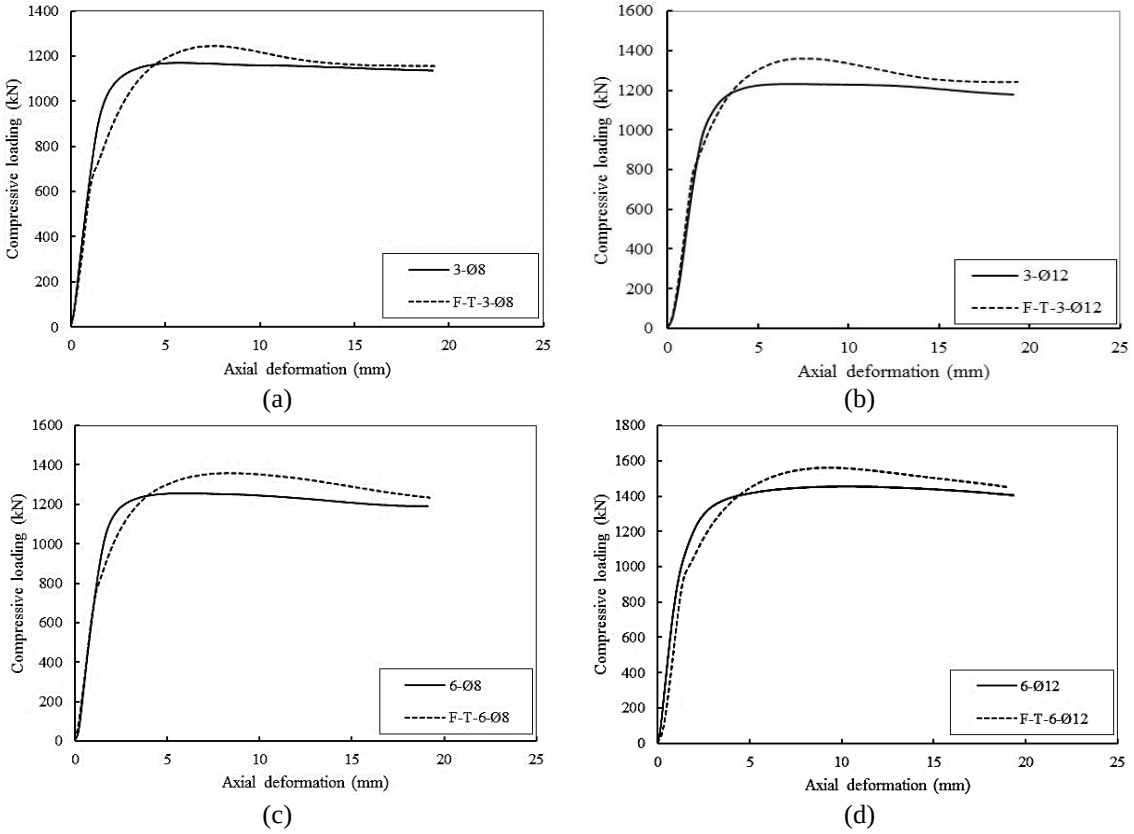

Fig. 10 Total applied load versus axial deflections for columns with 3.15 mm steel wall thickness: (a) 3-Ø 8 and F-T-3-Ø 8; (b) 3-Ø 12 and F-T-3-Ø 12; (c) 6-Ø 8 and F-T-6-Ø 8; and (d) 6-Ø 12 and F-T-6-Ø 12 columns tested both before and after fire exposure

In order to evaluate the initial stiffness of the columns, Eq. (1) for initial stiffness was developed based on the displacement δ_y and load capacity P_y at yield point (Choi and Park (2013), as show in Fig. 12.

$$K_i = \frac{P_y}{\delta_y} \tag{1}$$

Thus, it can be concluded that all specimens exposed to high temperatures exhibited higher compression capacity, lower stiffness and lower ductility when compared with unheated specimens as shown in Figs. 10, 11 and 12. The ratios of the failure load of all tested specimens after exposure to high temperatures to those of their corresponding unheated specimens ($N_{test}/N_{ambient}$) are listed in Table 2.

3.3 Failure modes

3.3.1 General observations after fire exposure

After exposure to the fire test, the two specimens incorporating no reinforcing bars behaved completely differently from the rest eight specimens. The concrete cores of these two specimens

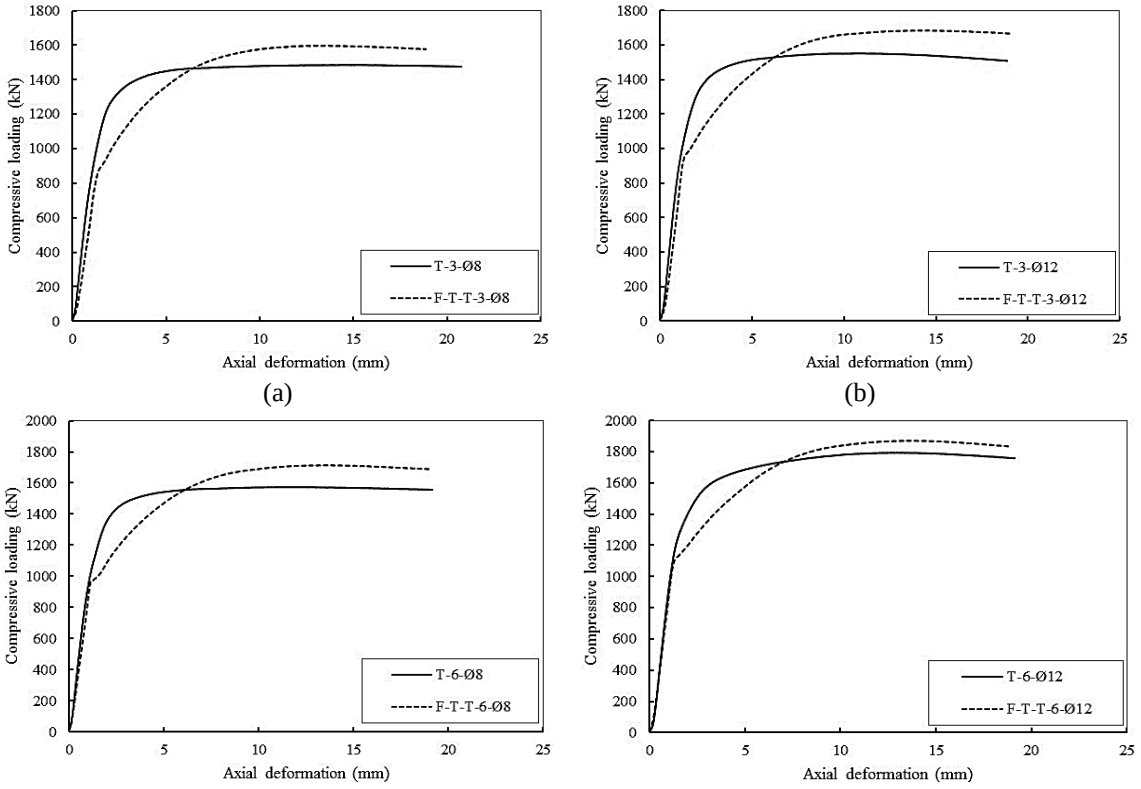

Fig. 11 Applied load versus axial deformation for columns with 5.63 mm steel wall thickness:(a) T-3-Ø 8 and F-T-T-3-Ø 8; (b) T-3-Ø 12 and F-T-T-3-Ø 12; (c) T-6-Ø 8 and F-T-T-6-Ø 8; and (d) T-6-Ø 12 and F-T-T-6-Ø 12 columns tested both before and after fire exposure

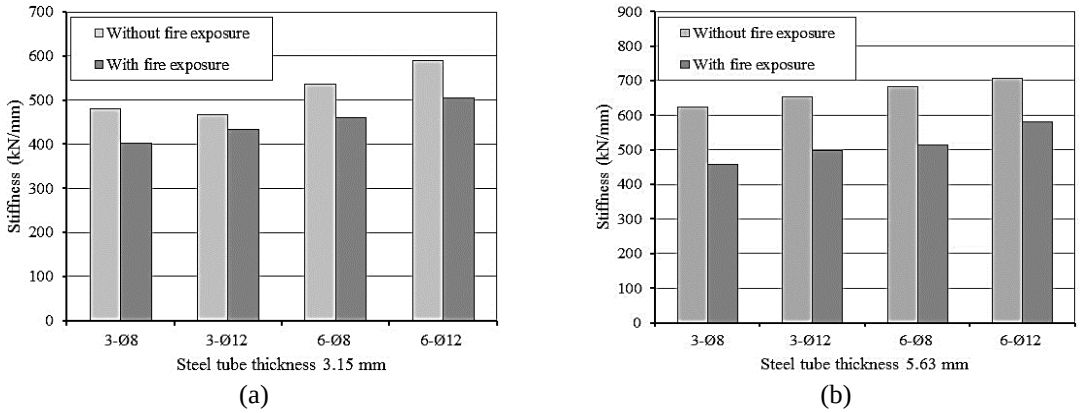

Fig. 12 Effect of temperature on stiffness: (a) for 3.15 mm wall thickness, and (b) for 5.63 mm wall thickness subjected to the smouldering fire test

suffered dramatic changes under fire exposure, where the core concrete cylinder was exploded approximately at its mid-height leading to the slipping of the upper half upward out of the steel

Table 2 Recorded loads and deflections at peak load measured during post-fire tests

Column no.	Test data		RSI		
	N_{test} (kN)	Axial deflection (mm)	$N_{ambient}$ (kN)	Axial deflection (mm)	$N_{test}/N_{ambient}$
F-T-3-Ø 8	1243	7.6	1170	5.8	1.06
F-T-6-Ø 8	1361	7.7	1257	5.2	1.08
F-T-3-Ø 12	1357	8.4	1230	6.8	1.10
F-T-6-Ø 12	1560	9.2	1455	10.5	1.07
F-T-T-3-Ø 8	1598	13	1486	15.2	1.07
F-T-T-6-Ø 8	1717	13.5	1573	11.5	1.09
F-T-T-3-Ø 12	1683	14.2	1554	10.7	1.08
F-T-T-6-Ø 12	1869	13.5	1796	12.6	1.04

*Test data: Results at peak load for load and axial deflection; RSI: Residual strength index.

(a) F-T-C (b) F-T-T-C

Fig. 13 Failure modes of specimens without reinforcing bars (F-T-C and F-T-T-C) during exposure to the smouldering fire test

tube as shown in Fig. 13. This behavior can be attributed to the continuously increased pore pressure due to the increasing of pore water evaporation under high temperature exposure. The examination of the failed specimens showed that concrete was completely crushed at the region of explosion. Oppositely, the specimens with welded reinforcing bars showed more stable behavior under fire exposure without showing any signs of explosion or noticeable deterioration. This behavior can be attributed to the presence of the steel bars, which significantly improved the thermal response of the composite columns under fire conditions.

3.3.2 General observations after compression tests

Figs. 14 and 15 shows that a typical failure mode of the steel tube was local outward folding failure. This is the same as that observed by some other researchers for CFST after exposure to elevated temperatures and at ambient temperatures (Han *et al.* 2005, Schneider 1998). Fig. 16 shows the measured compression loading versus longitudinal strain curves for the stub columns. The test results show that the axial load in the columns had remarkable effect on the mechanical behavior of the CFST stub columns after exposure to elevated temperatures. The higher the axial load level, the larger the residual deformations that the columns had suffered. During the

(a) F-T-3-Ø 8 (b) F-T-3-Ø 12 (a) F-T-6-Ø 8 (d) F-T-6-Ø 12

Fig. 14 Failure modes of column specimens with 3.15 mm wall thickness exposed to the smouldering fire test after compression loading

(a) F-T-T-3-Ø 8 (b) F-T-T-3-Ø 12 (c) F-T-T-6-Ø 8 (d) F-T-T-6-Ø 12

Fig. 15 Failure modes of column specimens with 5.63 mm wall thickness exposed to the smouldering fire test after compression loading

compression loading test, the steel tubes of most columns were firstly found to plump up at the middle height of the specimen after they experienced the elasto-plastic stage and/or the peaks of the compression loading. Subsequently the steel tube of column at one end plumped up as shown in Figs. 14 and 15. It is known that the presence of concrete in CFST stub columns changes the behavior of the steel tube and buckling mode at ambient temperatures (Uy 1998). The present specimen tests showed that concrete also changes the behavior of the steel tube and the buckling mode in the CFST stub columns at elevated temperatures. The buckling mode of the steel tube in the CFST stub columns at elevated temperatures is similar to that at ambient temperatures. In addition, it was found that stub columns retained integrity and there was no separation between the steel tube with welded reinforcing bars and concrete after test. This implies that there is an interaction between the concrete, welded reinforcing bars and the steel tube during the full course of heating. Furthermore, failure modes of the columns are very important in the performance evaluation of CFST specimens.

From the above analysis in the section 3.3.2, it is clear that there is a load transfer between the concrete and steel tube in the CFST stub columns after fire exposure. Ultimate compressive

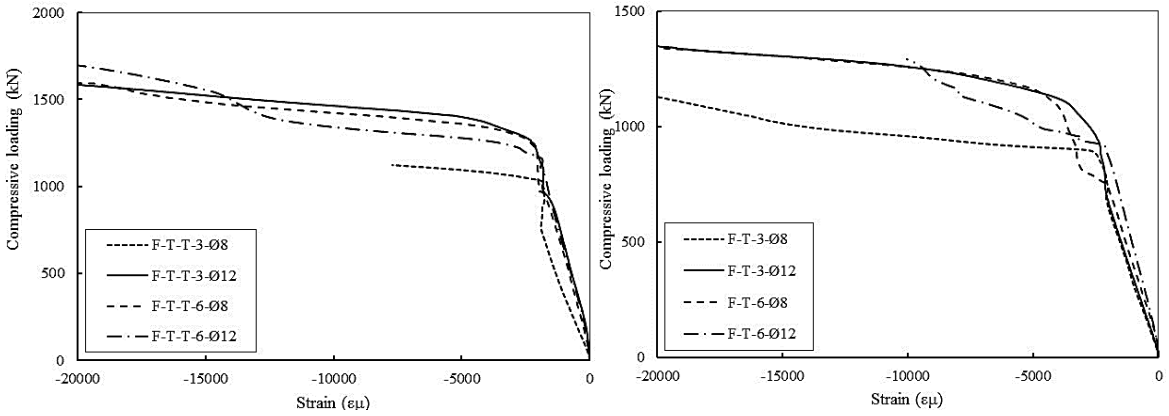

Fig. 16 longitudinal strains of the steel tubes: (a) with 3.15 mm wall thickness, and (b) with 5.63 mm wall thickness

strength of the core concrete in the inner part of the concrete degrades slowly after fire exposure in this part of concrete. The concrete can continuously take compressive loads transferred from the steel until the outer part of the concrete reaches its compressive strength (Lu *et al*. 2009). On the other hand, the concrete provides lateral support for the steel so it can retain its load capacity to some extent when the steel buckles locally. The interaction between the concrete and steel in the CFST stub columns is a key factor responsible for the good fire performance of the columns.

There exist a few variations between failure of specimens with 3.15 mm and 5.63 mm tube thicknesses. However, outward local buckling of the steel tube was observed in all columns with fire exposure. Moreover, the crippling type of failure happened in the specimens with thinner tubes, in column F-T-6-Ø 8 as an example as show in Fig. 14. Such behavior was not observable in columns with thicker tubes.

4. Influence of different parameters

4.1 Effect of steel tube thickness

Fig. 17 shows the observed compressive loading versus axial deformation for groups of identical specimens but with different steel tube thicknesses. Specimens with 5.63 mm tube thickness exhibited better performance. It can be observed in Fig. 17 that the increase of the tube wall thickness led to superior ductility, higher toughness and higher initial stiffness. Compression load capacities of columns F-T-T-3-Ø 8, F-T-T-3-Ø 12, F-T-T-6-Ø 8 and F-T-T-6-Ø 12 were 1598.7, 1683, 1717.2 and 1869.4 kN, respectively. Considering the CFST stub columns with fire exposure, thicker steel tubes with 3Ø 8 mm reinforcing bars exhibited 28.6% greater compression capacity compared to their corresponding thinner walled specimens. Considering the corresponding unheated specimens (T-3-Ø 8 and 3-Ø 8), the load capacity of the thicker steel tube was 27% higher than that of the thinner tube specimen. Similar trend of results was observed for the other reinforcement configurations, both for the heated and unheated specimens.

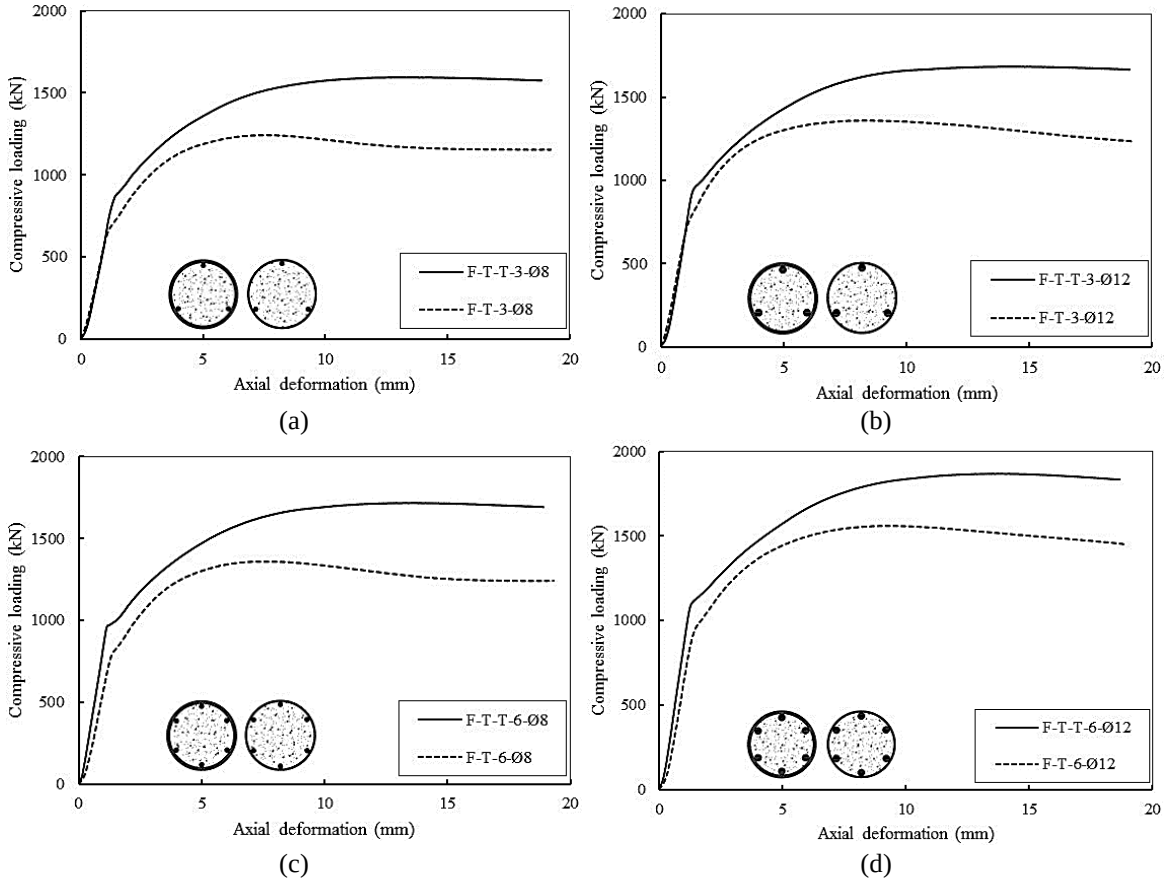

Fig. 17 Effect of steel tube thickness on residual compressive loading versus axial deformation response of CFST stub columns: (a) F-T-T-3-Ø 8 and F-T-3-Ø 8; (b) F-T-T-3-Ø 12 and F-T-3-Ø 12; (c) F-T-T-6-Ø 8 and F-T-6-Ø 8; and (d) F-T-T-6-Ø 12 and F-T-6-Ø 12

4.2 Effect of the diameter of the reinforcing bars

Fig. 18 shows that the increase of the diameter of the welded reinforcing bars increases the compression capacity of the columns. The comparisons shown in the figure reveal that the bar diameter is an effective parameter on the CFST behavior both before and after exposure to high temperatures. For the CFST with thin steel tubes and exposed to high temperatures, the increasing of the diameter of the six welded reinforcing bars from 8 mm to 12 mm led to 14.7% capacity improvement (F-T-6-Ø 12 compared to F-T-6-Ø 8).

4.3 Effect of the number of the reinforcing bars

Fig. 19 shows a higher peak compression capacity for the specimens with higher number of welded reinforcing bars. For the heated specimens incorporating thin walled steel tubes and 12 mm diameter bars, the duplication of the number of bars from 3 to 6 led to 15% increase in load capacity (comparison of F-T-3-Ø 12 and F-T-6-Ø 12). Similar load capacity improvements were

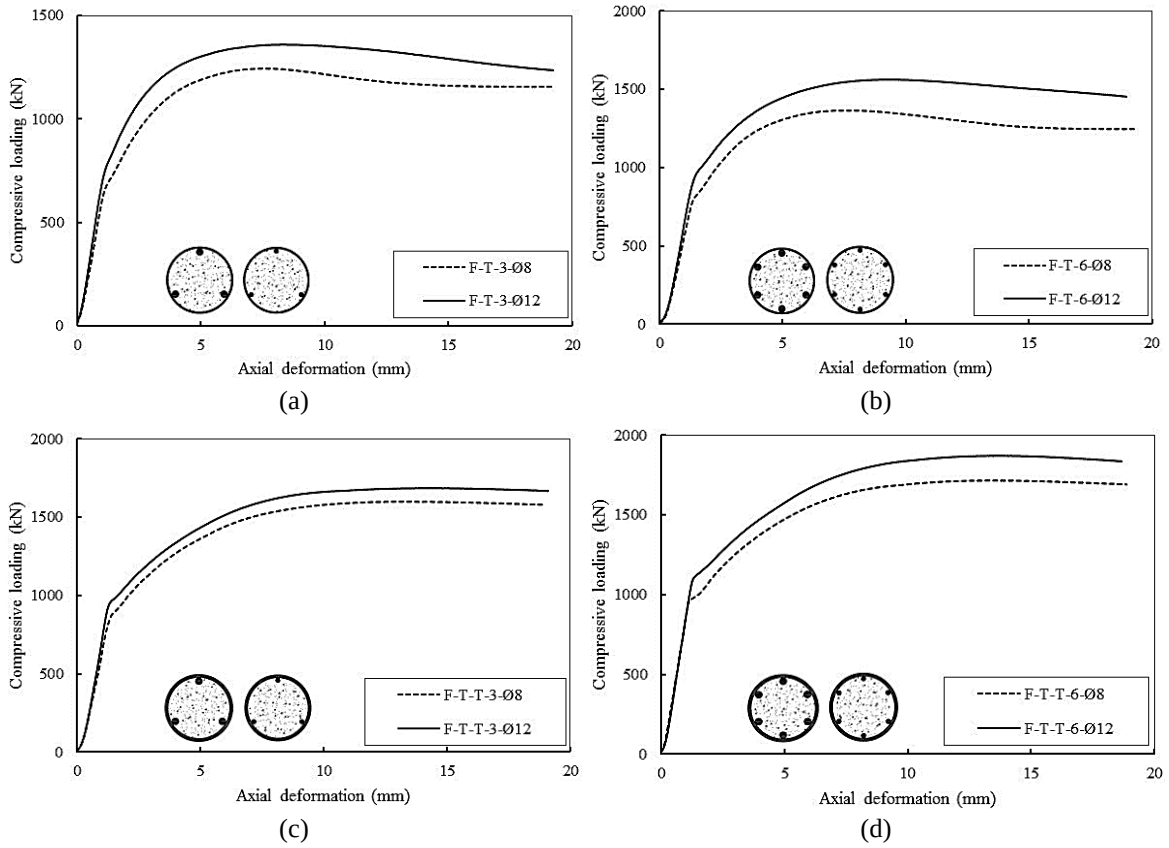

Fig. 18 Effect of the reinforcing bar diameter on the residual compressive loading versus axial deformation response of CFST stub columns: (a) F-T-3-Ø 8 and F-T-3-Ø 12; (b) F-T-6-Ø 8 and F-T-6-Ø 12; (c) F-T-T-3-Ø 8 and F-T-T-3-Ø 12; and (d) F-T-T-6-Ø 8 and F-T-T-6-Ø 12

achieved for the other bar diameters and wall thicknesses, both for the heated and unheated specimens. In general, comparing two identical specimens with different number of bars, the specimens with six bars gave from 7 to 15% higher load capacity compared to those with only three bars.

5. Design specifications

Design specifications support researchers and engineers to predict the capacities of the different structural columns. For composite columns made of concrete and steel, Eurocode-4 (EC4) (2004) and AISC 360-10 (2010) are well practiced design specifications around the world. For this reason, AISC 360-10 and EC4 are utilized in this paper.

5.1 AISC 360-10

For axially loaded circular CFST specimens, AISC 360-10 utilize Eq. (2) to compute

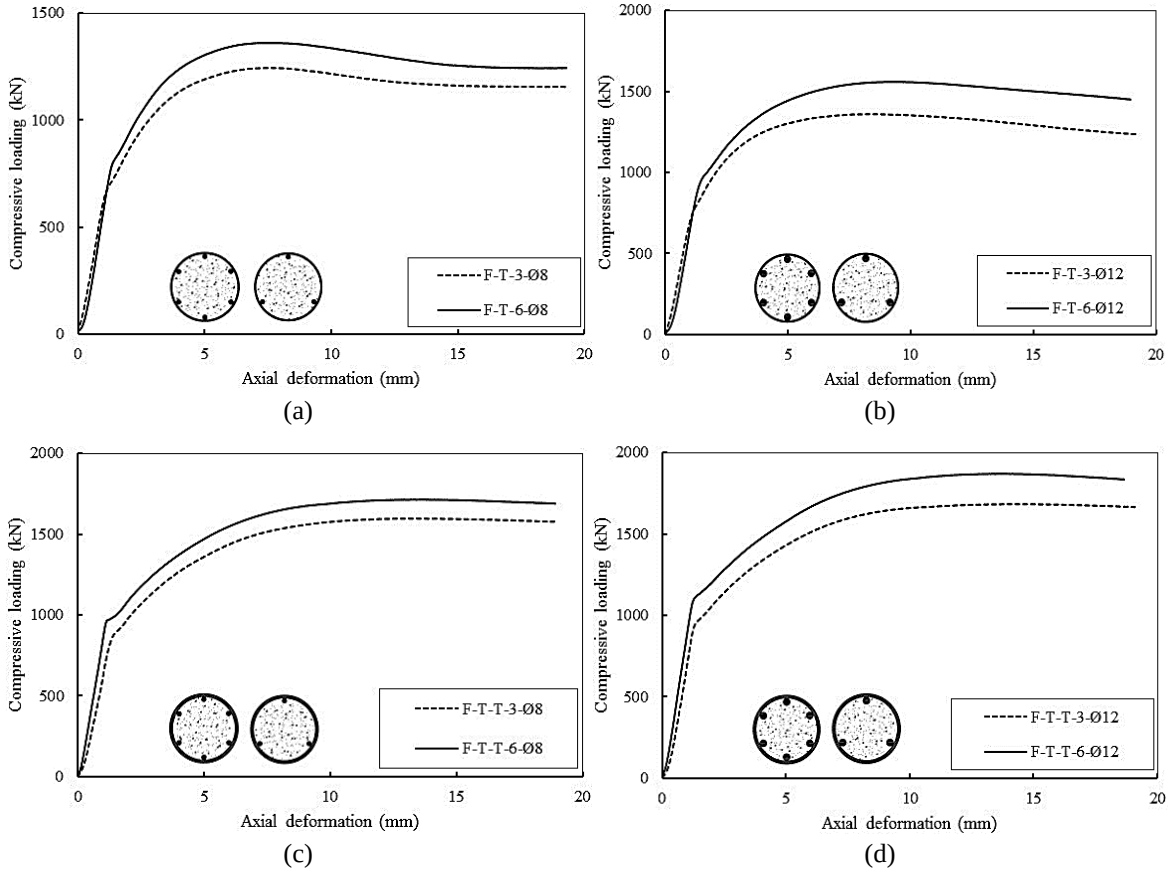

Fig. 19 Effect of reinforcing bars number on the residual compressive loading versus axial deformation response of CFST stub columns: (a) F-T-3-Ø 8 and F-T-6-Ø 8; (b) F-T-3-Ø 12 and F-T-6-Ø 12; (c) F-T-T-3-Ø 8 and F-T-T-6-Ø 8; and (d) F-T-T-3-Ø 12 and F-T-T-6-Ø 12

compression load capacity as follows

$$\begin{aligned} P_n &= P_{n0}\left[0.658^{\frac{P_{n0}}{P_e}}\right] && \frac{P_{n0}}{P_e} \leq 2.25 \\ P_n &= 0.877P_e && \frac{P_{n0}}{P_e} > 2.25 \end{aligned} \tag{2}$$

where (P_{n0}) refers to the compressive capacity of the composite column and (P_e) refers to Euler critical load of the composite column, which is determined utilizing effective stiffness EI_{eff}

$$EI_{eff} = E_s I_s + E_s I_{sr} + C_3 E_c I_c \tag{3}$$

Modulus of elasticity of concrete in AISC 360-10 is given by $(E_c) = 4700\sqrt{f_c'}$ and C_3 is the (coefficient for effective rigidity) of the filled composite member

$$C_3 = 0.6 + 2\left[\frac{A_s}{A_c + A_s}\right] \leq 0.9 \tag{4}$$

AISC standards consider local buckling influence utilizing three various classifications for tubes. The circular composite column is considered to be (compact) if D/t ratio is smaller than $\lambda_p = 0.15\,E_s/F_y$. The section is considered to be (slender) when D/t ratio is larger than $\lambda_r = 0.19\,E_s/F_y$. Finally, the section is considered to be (non-compact) if D/t ratio is smaller than λ_r but larger than λ_p. The compressive load capacity of the section P_{n0} is computed based on these classifications of sections. For compact composite sections, the compressive load capacity P_{n0} is equal to the plastic strength of the composite column P_p

$$P_{n0} = P_p \tag{5}$$

Plastic strength of the composite column is given by

$$P_p = F_y A_s + C_2 f_c' \left[A_c + A_{sr}\frac{E_s}{E_c}\right] \tag{6}$$

For circular columns, C_2 is equal to (0.95). Based on this coefficient, AISC standard implies that the tube of the composite column reaches to yield strength when the strength of the concrete is about $0.95f_c'$. The parameter C_2 is equal to (0.85) for rectangular and square composite columns. AISC standard considers the confinement influence of circular tube by only incorporating C_2 coefficient of (0.95), instead of (0.85), which means an (11%), stable performance increase for circular steel tubes.

For (slender sections), the compressive load capacity is computed as follows

$$P_{n0} = F_{cr} A_s + 0.7 f_c' \left[A_c + A_{sr}\frac{E_s}{E_c}\right] \tag{7}$$

In Eq. (7) F_{cr} of the steel tube refers to stress of critical local buckling of the CFST column, and is formulated as follows

$$F_{cr} = \frac{0.72F_y}{\left(\left(\frac{D}{t}\right)\frac{F_y}{E_s}\right)^{0.2}} \tag{8}$$

In these AISC equations and formulas, (slender sections) are required to develop and improve critical local buckling stress $0.7f_c'$ of the core concrete and f_{cr} of the steel tube.

For (non-compact sections), the compressive load capacity is given as follows

$$P_{n0} = P_p - \frac{P_p - P_y}{(\lambda_r - \lambda_p)^2}(\lambda - \lambda_p)^2 \tag{9}$$

In Eq. (9) P_y refers to the yield strength of the circular column and is calculated as follows

$$P_y = F_y A_s + 0.7 f_c' \left[A_c + A_{sr}\frac{E_s}{E_c}\right] \tag{10}$$

5.2 Eurocode-4

The plastic resistance of a CFST section is computed by adding the resistances of concrete, steel tube and reinforcement bars as follows

$$N_{pl,Rd} = A_a f_y + A_c f_c + A_s f_s \tag{11}$$

Rectangular and square steel tubes offering little confinement due to the walls of these steel tubes should resist the pressure of concrete by plate bending, rather than generating hoop stresses in circular composite columns (Alostaz and Schneider 1996). For the circular composite sections, EC4 offers an explicit equation which incorporates the confinement influence as follows

$$N_{pl,Rd} = \eta_a A_a f_y + A_c f_c \left(1 + \eta_c \frac{t}{d}\frac{f_y}{f_c}\right) + A_s f_s \tag{12}$$

where η_a refers to the steel tube reduction factor and η_c refers to the concrete core enhancement factor. If the eccentricity is lower than (10%) of the outer D of the tube, the concrete enhancement factor and the steel reduction factor are determined as follows

$$\eta_a = 0.25\left(3 + 2\bar{\lambda}\right) \leq 1.0 \tag{13}$$

$$\eta_c = 4.9 - 18.5\bar{\lambda} + 17\bar{\lambda}^2 \geq 0 \tag{14}$$

EC4 standards consider the confinement influence in CFST specimens when the relative slenderness $\bar{\lambda}$ not exceeds (0.5).

$$\bar{\lambda} = \sqrt{\frac{N_{pl,Rd}}{N_{cr}}} \tag{15}$$

in which $N_{pl,Rd}$ refers to the plastic resistance of the composite column, determined by using Eq. (11) and N_{cr} refers to Euler critical normal force. A critical force of the column is calculated as follows

$$N_{cr} = \frac{\pi^2 (EI)_{eff}}{(L)^2} \tag{16}$$

where $(EI)_{eff}$ is the effective stiffness which is calculated as follows

$$(EI)_{eff} = E_a I_a + E_s I_s + K_e E_{cm} I_c \tag{17}$$

where E_a refers to the elastic modulus of steel tube, E_s refers to the elastic modulus of steel reinforcement and E_{cm} refers to the elastic modulus of concrete, which is given by

$$E_{cm} = 22000 \left(\frac{f_{ck} + 8MPa}{10}\right)^{0.3} \tag{18}$$

where I_a, I_s and I_c are the moment of inertia of steel tube, the reinforcement and the concrete, respectively. Finally, K_e refers to the correction coefficient equals to (0.6). Also, EC4 standards consider the influences of disadvantages that may cause second order moments by multiply the reduction factor (χ) with the column plastic resistance, where

$$\chi = \frac{1}{\phi + \left[\phi^2 - \bar{\lambda}^2\right]^{0.5}} \leq 1.0 \tag{19}$$

The parameter ϕ is determined as follows

$$\phi = 0.5\left[1 + \alpha\left(\bar{\lambda} - 0.2\right) + \bar{\lambda}^2\right] \tag{20}$$

where α refers to the imperfection coefficient, which is equal to (0.21) for CFST specimens.

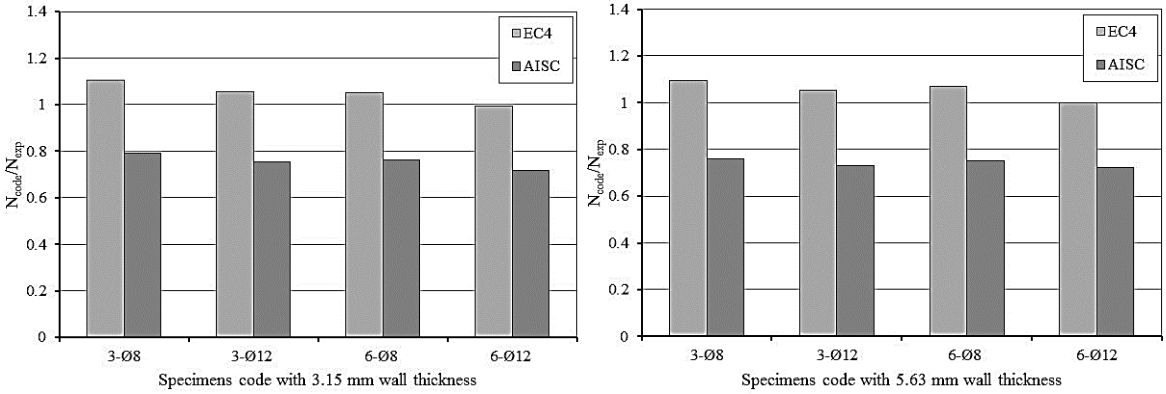

(a) (b)

Fig. 20 Predicted-to-experimental column strengths considering different codes predictions: (a) with 3.15 mm wall thickness, and (b) with 5.63 mm wall thickness

Table 3 Experimental results and code predictions

Column no.	N_{exp} (kN)	N_{EC4} (kN)	P_{AISC} (kN)	N_{EC4}/N_{exp}	P_{AISC}/N_{exp}
F-T-3-Ø 8	1243.380	1371.816	9851.486	1.103296	0.792315
F-T-6-Ø 8	1361.010	1434.491	1023.602	1.053993	0.752093
F-T-3-Ø 12	1357.570	1429.263	1033.163	1.052812	0.761039
F-T-6-Ø 12	1560.590	1559.310	1119.210	0.999179	0.717171
F-T-T-3-Ø 8	1598.730	1746.870	1217.411	1.092661	0.761486
F-T-T-6-Ø 8	1717.230	1804.792	1255.291	1.050995	0.730998
F-T-T-3-Ø 12	1683.010	1798.428	1264.711	1.068578	0.751458
F-T-T-6-Ø 12	1869.410	1870.061	1349.979	1.000348	0.722142
			Mean	1.051930	0.748587

*N_{EC4}: Plastic resistance; P_{AISC}: Nominal strength

Many previous researchers compared the predicted strengths calculated using the two adopted standards with their experimental works and show different conclusions.

Ding *et al*. (2011) compared experiment results of 115 specimens with AISC 360-10 standard predictions and showed that AISC 360-10 standard predictions can be relatively conservative by approximately (36.6%). On the other hand, they showed that EC4 standard predictions are in perfect agreement with the experiment results of short specimens. The maximum conservative expectation of EC4 standards for short specimens was (17.2%). On the other hand, overestimated expectation of EC4 standards for long and short specimens were reported by Oliveira *et al*. (2009). They reported that the predictions of the AISC standards for long specimens are very superior compared to short specimen.

In the present paper, AISC and EC4 were used and test results were compared with the predictions of these design specifications as shown in Table 3. Since AISC 360-10 and EC4 have no special formulations for vertically welded reinforcing bars inside steel tube, calculations were carried out considering that the reinforcing bars are not welded to the steel tube. In addition, the materials properties were used in the predictions of design specifications AISC and EC4 after exposure to high temperatures. The predictions of AISC 360-10 were found to be conservative for

the tested specimens. On the other hand, the test results were found to be very close to the predictions of EC4, especially for F-T-6-Ø 12 and F-T-T-6-Ø 12 columns. However, for F-T-6-Ø 12 column, EC4 resulted in slightly conservative prediction compared to the test results. For the specimens F-T-3-Ø 8, F-T-6-Ø 8, F-T-3-Ø 12, F-T-T-3-Ø 8, F-T-T-6-Ø 8, F-T-T-3-Ø 12 and F-T-T-6-Ø 12, EC4 gave slightly unconservative predictions, yet these predictions still closer to the experimental results than those of AISC 360-10. The ultimate strength (N) was compared with AISC and EC4 predictions of design specifications, as shown in Fig. 20.

In the current computations, all safety factors of EC4 and AISC 360-10 were set to unity. Material safety factors in EC4 are 1.5 and 1.0 for concrete and steel tube, respectively. On the other hand, AISC computations do not include material safety factors. Instead, AISC 360-10 applies member resistance factor of 0.75 to computed capacity of specimen (Ekmekyapar 2016). Generally, the application of the material safety factors for predictions of EC4 standard would result in reasonable and logical designs even for most unconservative EC4 predictions. Furthermore, the application of the resistance factor for predictions of AISC would lead to conservative designs compared to the design results of EC4. Mean values of the ratios of code prediction to test result confirm this phenomenon

6. Conclusions

The post-fire behavior of the axially loaded CFST stub columns has been investigated experimentally. The experimental work of this research includes the fabrication and testing of 20 composite column specimens. The analysis and results of eight post-fire residual axial compressive loading tests of CFST stub columns are presented and discussed. On the other hand, ten specimens were loaded axially without fire exposure, while two specimens were failed during exposure to the fire. Based on the test and analysis results of this work, the following conclusions can be drawn.

- Considering the CFST stub columns with fire exposure, thicker steel tubes with 3Ø 8 mm reinforcing bars exhibited 28.6% greater compression capacity compared to their corresponding thinner walled specimens. Considering the corresponding unheated specimens (C and T-C), the load capacity of the thicker steel tube was 28.1% higher than that of the thinner tube specimen.
- The diameter and number of welded reinforcing bars significantly improves the toughness, ductility and compression performance of the columns. The improvements are much more perceptible in columns without fire exposure led to 37.2% capacity improvement (comparison of C and 6-Ø 12), whereas it increases the performance by 25.6% in the columns with fire exposure (comparison of F-T-3-Ø 8 and F-T-6-Ø 12).
- Two specimens without welded reinforcing bars were found to have concrete burst during the fire exposure owing to the pressure of water vapor in the concrete core. The tests showed that the columns without reinforcing bars may be unsafe during the exposure to the fire. Thus, structural engineers and researchers should pay more attention to the selection of suitable concrete and determination of details of vent holes in the concrete core.
- Considering different (*D/t*) ratios utilized in this research, it has been shown that welded reinforcing bars can be used for thicker and thinner steel tubes which are filled with concrete. Nevertheless, further experimental studies are required considering different *D/t* ratios to assess the performance of the welded reinforcing bars performance for wider range of investigated parameters before, during and after exposure to the fire.
- Using vertically welded reinforcing bars in CFST stub column applications would result in

cost effective and reliable designs, provided that a suitable weld plan is followed.

• It is worth to note here, that the use of type F fly ash enhances the compressive strength of concrete after exposure to high temperatures. In this research, where the used concrete incorporates type F fly ash, it was found that the load resistances of specimens exposed to 750℃ were higher than those of corresponding unheated specimens, the reason was type F fly ash increasing compression load capacity of CFST stub columns.

References

Ada, M., Sevim, B., Yuzer, N. and Ayvaz, Y. (2018), "Assessment of damages on a RC building after a big fire", *Adv. Concrete Constr.*, **6**(2), 177-197.

AISC 360-10 (2010), Specification for Structural Steel Buildings, American Institute of Steel Construction, Chicago, USA

Alostaz, Y.M. and Schneider, S.P. (1996), "Connections to concrete-filled steel tubes", Department of Civil Engineering, University of Illinois, Urbana Champaign.

ASTM C39/C39M-14 (2014), Standard Test Method for Compressive Strength of Cylindrical Concrete Specimens, ASTM International, West Conshohocken, PA 19428-2959, United States.

CEN. BS EN 13381-8:2010 (2010), Test Method for Determining the Contribution to the Structural Fire Resistance of Structural Members, Part 8: Applied Reactive Protection to Steel Members, Brussels, Belgium.

Choi, E.G., Kim, H.S. and Shin, Y.S. (2012), "Performance of fire damaged steel reinforced high strength concrete (SRHSC) columns", *Steel Compos. Struct.*, **13**(6), 521-537.

Choi, S.M. and Park, J.W. (2013), "Structural behavior of CFRP strengthened concrete-filled steel tubes columns under axial compression loads", *Steel Compos. Struct.*, **14**(5), 453-472.

Ding, F.X., Yu, Z.W., Bai, Y. and Gong, Y.Z. (2011), "Elasto-plastic analysis of circular concrete-filled steel tube stub columns", *J. Constr. Steel. Res.*, **67**, 1567-1577.

EC4 (2004), Eurocode 4: Design of Composite Steel and Concrete Structures, Part 1-1: General Rules and Rules for Buildings, British Standards Institution, London, UK.

Ekmekyapar, T. (2016), "Experimental performance of concrete filled welded steel tube columns", *J. Constr. Steel. Res.*, **117**, 175-84.

Ekmekyapar, T. and Al-Eliwi, B.J.M. (2016), "Experimental behavior of circular concrete filled steel tube columns and design specifications", *Thin Wall. Struct.*, **105**, 220-30.

Ekmekyapar, T. and AL-Eliwi, B.J.M. (2017), "Concrete filled double circular steel tube (CFDCST) stub columns", *Eng. Struct.*, **135,** 68-80.

Han, L.H. (2001), "Performance-based fire resistance design of concrete-filled steel columns", *J. Constr. Steel. Res.*, **57**(6), 697-711.

Han, L.H. and Huo, J.S. (2003), "Concrete filled hollow structural steel columns after exposure to ISO-834 standard fire", *J. Struct. Eng.*, **129**(1), 68.

Han, L.H., Huo, J.S. and Wang, Y.C. (2005), "Compressive and flexural behavior of concrete filled steel tubes after exposure to standard fire", *J. Constr. Steel. Res.*, **61**(7), 882-901.

Han, L.H., Yang, Y.F., Yang, H. and Huo, J.S. (2002), "Residual strength of concrete-filled RHS columns after exposure to the ISO-834 standard fire", *Thin Wall. Struct.*, **40**(12), 991-1012.

Ibrahim, R.K.H., Hamid, R. and Taha, M.R. (2012), "Fire resistance of high-volume fly ash mortars with nanosilica addition", *J. Constr. Build. Mater.*, **36**, 779-786.

Kim, DK., Choi, SM. and Chung, K.S. (2000), "Structural characteristics of CFT columns subjected fire loading and axial force", *Proceedings of the 6th ASCCS Conference*, Los Angeles, USA.

Kodur, V.K.R. (1999), "Performance-based fire resistance design of concrete-filled steel columns", *J. Constr. Steel. Res.*, **51**(1), 21-6.

Kodur, V.K.R. and Sultan, M.A. (2000), "Enhancing the fire resistance of steel columns through composite

construction", *Proceedings of the 6th ASCCS Conference,* Los Angeles, CA.
Lu, H., Zhao, X.L. and Han, L.H. (2009), "Fire behaviour of high strength self-consolidating concrete filled steel tubular stub columns", *J. Constr. Steel. Res*., **65**, 1995-2010.
Oliveira, W.L.A.D., Nardin, S.D., Debs, A.L.H.D.C.E. and Debs, M.K.E. (2009), "Influence of concrete strength and length/diameter on the axial capacity of CFT columns", *J. Constr. Steel. Res*., **65**, 2103-2110.
Park, S.H., Choi, S.M. and Chung, K.S. (2008), "A Study on the fire-resistance of concrete-filled steel square tube columns without fire protection under constant central axial loads", *Steel Compos. Struct*., **8**(6), 491-510.
Rashad, A.M. and Zeedan, S.R. (2011), "The effect of activator concentration on the residual strength of alkali-activated fly ash pastes subjected to thermal load", *J. Constr. Build. Mater*., **25**, 3098-3107.
Renaud, C., Aribert, J.M. and Zhao, B. (2003), "Advanced numerical model for the fire behavior of composite columns with hollow steel section", *Steel Compos. Struct*., **3**(2), 75-95.
Rush, D., Bisby, L., Jowsey, A., Melandinos, A. and Lane, B. (2012), "Structural performance of unprotected concrete-filled steel hollow sections in fire", *Steel Compos. Struct*., **12**(4), 325-352.
Schneider, S.P. (1998), "Axially loaded concrete-filled steel tubes", *J. Struct. Eng*., **124**(10), 1125-1138
Shaikh, F.U.A. and Taweel, M. (2015), "Compressive strength and failure behaviour of fibre reinforced concrete at elevated temperatures", *Adv. Concrete Constr.*, **3**(4)**,** 283-293.
Tao, Z., Uy, B., Han, L.H. and Wang, Z.B. (2009), "Analysis and design of concrete-filled stiffened thin-walled steel tubular columns under axial compression", *Thin Wall. Struct*., **47**(12), 1544-56.
Tao, Z., Wang, Z.B., Han, L.H. and Uy, B. (2011), "fire performance of concrete-filled steel tubular columns strengthened by CFRP", *Steel Compos. Struct*., **11**(4), 307-324.
Uy, B. (1998), "Local and post-buckling of concrete filled steel welded box columns", *J. Constr. Steel. Res*., **47**(12), 47-72.
Yang, H., Han, L.H. and Wang, Y.C. (2008), "Effects of heating and loading histories on post-fire cooling behavior of concrete-filled steel tubular columns", *J. Constr. Steel. Res*., **64**(5), 556-70.
Zaharia, R. and Dubina, D. (2014), "fire design of concrete encased columns: Validation of an advanced calculation model", *Steel Compos. Struct*., **17**(6), 835-850.
Zhang, B., Cullen, M. and Kilpatrick, T. (2014), "Fracture toughness of high performance concrete subjected to elevated temperatures Part 1 The effects of heating temperatures and testing conditions (hot and cold)", *Adv. Concrete Constr.*, **2**(2), 145-162.
Zhang, B., Cullen, M. and Kilpatrick, T. (2016), "Spalling of heated high performance concrete due to thermal and hygric gradients", *Adv. Concrete Constr.*, **4**(1)**,** 001-014.
Zhang, H.Y., Kodur, V., Qi, S.L., Cao, L. and Wu, B. (2014), "Development of metakaolin–fly ash based geopolymers for fire resistance applications", *J. Constr. Build. Mater*., **55**, 38-45.
Ziemian, R.D. (2010), Guide to Stability Design Criteria for Metal Structures, 6th Edition, Wiley.

CC

Nomenclature

A_a	cross-sectional area of steel tube using theEurocode
A_c	cross-sectional area of concrete
A_s	cross-sectional area of steel tube using theAISC Standard
A_s	cross-sectional area of steel reinforcement using the Eurocode
A_{sr}	cross-sectional area of steel reinforcement
C_3	coefficient for effective rigidity
D	diameter of the circular steel tube

E_a elastic modulus of steel tube
E_c elastic modulus of concrete using the AI-SC Standard
E_{cm} elastic modulus of concrete using the Eur-ocode
EI_{eff} effective stiffness
E_s elastic modulus of steel reinforcement
F_{cr} critical stress
f_c cylinder compressive strength of oncrete
f_{ck} (Eurocode) characteristic compressive cyli-nder strength of concrete at 28 days
f_c' concrete cylinder strength using the AISCStandard
f_s yield strength of steel reinforcement
F_y yield strength of steel tube using the AI-SC Standard
f_y yield strength of steel tube
I_a moment of inertia of steel tube using theEurocode
I_c moment of inertia of concrete
I_s moment of inertia of steel tube using the AIS-C Standard
I_s moment of inertia of steel reinforcement usi-ng the Eurocode
I_{sr} moment of inertia of steel reinforcement
K_e correction coefficient
K_i initial stiffness
L length of member
$N_{pl,Rd}$ plastic resistance of the composite column
N_{cr} Euler critical normal force
P_e Euler critical load of the composite colu-mn
P_n compression load capacity
P_{n0} nominal axial strength
P_p plastic strength of the composite column
P_y yield strength of the circular column usin-g the AISC Standard
P_y load strength
t wall thickness of the steel tube
α imperfection coefficient
η_a steel tube reduction factor
η_c concrete core enhancement factor
δ_y displacement
λ slenderness ratio
λ_p elastic critical slenderness ratio
$\bar{\lambda}$ relative slenderness
ϕ $0.5\left[1+\alpha\left(\bar{\lambda}-0.2\right)+\bar{\lambda}^2\right]$
χ reduction factor